

DATA REPOSITORY ITEM DR2009146

SUPPLEMENTARY MATERIALS

Methods

Electron Microprobe. Biotite composition of Table DR1 and glass composition 1 in Table DR2: JEOL JXA-8200 of I.N.G.V. Roma, 15 kV accelerating voltage, 8 nA beam current, probe diameter 0.5 μm . Na, Si, K, Ca and Al analyzed as first elements, with counting times of 10 s on peak and 5 on background, and ZAF data correction.

Glass analyses 2-5 in Table DR2: Cameca SX50 of C.N.R.-I.G.G. Padova, 20 kV accelerating voltage, 7 nA beam current, Na, Si, K and Ca analyzed as first elements, counting times: 8 s on peak, 4 s on background for Na, 10 s on peak and 5 on background for other elements, and PAP data correction. Na loss in glass evaluated by analysis of a rhyolitic glass standard (Morgan and London, 2005) at the same working conditions, and verified to be <30% relative. The correction operated in Table DR2 (analyses 1*-5*) adopts a conservative factor of 40% relative and demonstrates that the very low Na content is a primary feature of the glassy inclusions.

Scanning Electron Microscopy. Jeol JSM-6500F thermal FESEM of I.N.G.V. Roma, 15 kV accelerating voltage, 8 nA probe current. X-ray mapping performed at Mag 4500X, resolution 1024*768 pixel, dwell time 2 ms (real time) per pixel.

Raman microspectroscopy. Home made micro-Raman system at the Department of Chemical Sciences, University of Padova, equipped with a liquid nitrogen cooled CCD detector and an Ar⁺ laser operating at 514.5 nm as excitation source, spectral resolution 2 cm^{-1} , spatial lateral resolution best than 0.5 μm , depth of focus between 1 and 2 μm . To avoid optical damage of the sample the irradiation power of the exciting radiation was maintained between 10 to 50 mW.

Experimental re-melting. Performed in a LINKAM TS1500 high temperature stage, using an inert atmosphere of He to prevent sample oxidation. Garnet fragments for re-melting are wafers <3-4 mm in diameter, obtained from 100 μm -thick doubly-polished sections of khondalite.

Supplementary Geological and Petrographic Information

The Kerala Khondalite Belt (KKB), belonging to the Southern India granulite terrain, is part of the Precambrian basement of India (Chacko et al., 1987; Santosh, 1986) and believed to have formed, with Madagascar and Sri Lanka, part of the Mozambique Belt of east Gondwana (Fig. DR1). The KKB exposes a regionally metamorphosed and melted deep crustal section and is an ideal case study of crustal scale anatexis of metasedimentary rocks. It comprises a sequence of granulite facies rocks that have migmatized to various extents (Chacko et al., 1992; Braun et al., 1996; Shabeer, 2004) and includes three major rock types: orthopyroxene-bearing charnockites, migmatized garnet-biotite-graphite-bearing gneisses (*leptynites*), and the most common garnet-sillimanite-graphite gneisses (*khondalites*). The latter are particularly widespread in the southern part of the KKB, also called Trivandrum Block and consist of Grt-Sil-Bt-Crd paragneisses (mineral abbreviations after Kretz, 1983) which underwent anatexis during the Pan-African event. The age of UHT metamorphism and partial melting has been determined between 590 and 550 Ma by U-Pb monazite dating (Cenki et al. 2004) and at 530 Ma by SHRIMP U-Pb zircon dating (Shabeer et al. 2005). The age of cooling below c. 400-500 °C has been determined at 490-470 Ma by Rb-Sr dating of biotite (Cenki et al. 2004).

The KKB rocks are examples of regional ultrahigh-temperature (UHT) metamorphism, i.e., at temperatures exceeding 900°C (Braun et al, 1996; Chacko et al., 1996; Nandakumar and Harley, 2000; Cenki et al., 2002; Tadokoro et al., 2008). The thermal peak, characterized by anatexis via the fluid-absent melting of biotite (Braun et al., 1996; Cenki et al., 2004), is not well constrained as concerns its pressure. Barometric estimates range from >5 kbar from Crd-bearing assemblages (Nandakumar and Harley, 2000) to >10 kbar from Spl+Qtz-bearing rocks (Tadokoro et al., 2008). The most accepted pressure range for the thermal peak, adopted also here, is 6-8 kbar (Cenki et al., 2004).

The studied khondalite samples were collected in the quarry of Koliakkode (Fig. DR1, coordinates N8 38' 24" E76 53' 30.5"), also studied by Tadokoro et al. (2008). Here, intensely folded stromatic

diatexites contain cm- to m-sized layers of Grt-Crd-rich khondalite constituting the melanosome (Fig. DR2). The khondalites have a medium to coarse grain-size, with folia of mm-sized sillimanite defining a foliation that anastomoses around garnet porphyroblasts. A typical reaction microstructure of these rocks is the partial replacement of garnet by cordierite (see also Nandakumar and Harley, 2000), that records near-isothermal decompressional along a clockwise path (Tadokoro et al., 2008). As a consequence, Crd-bearing equilibria do not record the P-T conditions of garnet formation and rock melting.

In the studied sample, garnet and cordierite form levels or elongated lenses along with minor amounts of quartz – normally hosted as small rounded grains in cordierite- and interstitial hercynite ± ilmenite. Garnet porphyroblasts are extensively fractured, and characterized by embayments due to replacement by cordierite. Cordierite is slightly oriented, locally pinitized, and easily recognizable from the pleochroic haloes around zircon inclusions. Cordierite and quartz locally occur within garnet fractures. K-feldspar occurs together with garnet and cordierite, showing two textural generations of perthites. Biotite is extremely rare in the matrix surrounding garnet, probably because it reacted out during dehydration melting.

The leucocratic portion of the sample is formed mainly of quartz and K-feldspar, and anastomoses around the garnet-cordierite-sillimanite portions.

Not all the garnet crystals of the melanosome host melt inclusions, and there is a sort of negative correlation between mineral inclusions and melt inclusions presence: the portions of garnet hosting melt inclusions are usually devoid of other inclusions, except for rare rounded biotite (probably the relicts left back by the dehydration melting reaction), and even more rare zircon and apatite. Conversely, melt inclusions are absent where garnet is rich in mineral inclusions. The latter consist mainly of oriented sillimanite needles and rounded to idiomorphic grains of biotite, plus minor quartz, ilmenite, apatite and zircon, and are arranged to define an internal foliation.

REFERENCES CITED

Braun, I., Raith, M. and Ravindra Kumar, G. R., 1996, Dehydration-melting phenomena in

- leptynitic gneisses and the generation of leucogranites: a case study from the Kerala Khondalite Belt, southern India: *Journal of Petrology*. v. 37, p. 1285–1305.
- Cenki, B., Kriegsman, L. M. and Braun, I., 2002, Melt-producing and melt-consuming reactions in anatectic granulites: P-T evolution of the Achankovil cordierite gneisses, South India: *Journal of Metamorphic Geology*, v. 20, p. 543-561.
- Chacko, T., Lamb, M. and Farquhar, J., 1996, in *The Archean and Proterozoic terrains in southern India within East Gondwana*. (eds Santosh, M. & Yoshida, M.) Gondwana Research Group Memoir 3. Field Science, 157–165, Osaka.
- Chacko, T., Ravindra-Kumar, G. R. and Newton, R. C., 1987, Metamorphic P-T conditions of the Kerala (S. India) Khondalite belt, a granulite facies supracrustal terrain: *Journal of Geology*. v. 95, p. 343–358.
- Chacko, T., Ravindra-Kumar, G. R., Meen, J. K. and Rogers, J. J. W., 1992, Geochemistry of high-grade supracrustal rocks from the Kerala Khondalite Belt and adjacent massif charnockites: *Precambrian Research*. v. 55, p. 469–489.
- Kretz, R., 1983, Symbols for rock-forming minerals: *American Mineralogist*. v. 68, p. 277-279.
- Santosh, M., 1986, Cordierite gneisses of southern Kerala, India: petrology, fluid inclusions and implications for crustal uplift history: *Contributions to Mineralogy and Petrology*. v. 96, p. 343–356.
- Shabeer, K. P., 2004, Petrology and geochronology of granulite facies metamorphic rocks from Kerala Khondalite Belt, southern India: implications to partial melting and heat source: Ph.D. thesis, Osaka City University, Osaka.
- Shabeer, K. P., Satish-Kumar, M., Armstrong, R. and Buick, I. S., 2005, Constraints on the timing of Pan-African granulite-facies metamorphism in the Kerala Khondalite Belt of southern India: SHRIMP mineral ages and Nd isotopic systematics: *Journal of Geology*. v. 113, p. 95-106.
- Tadokoro, H., Tsunogae, T. and Santosh, M., 2008, Metamorphic P-T path of the eastern Trivandrum Granulite Block, southern India: implications for regional correlation of lower

Table DR1. EMP analyses of biotite from nanogranite inclusions.

Id.	MI225_1	MI226_2	MI229
FeO	9.25	9.10	7.16
Na ₂ O	0.17	0.10	0.07
MgO	16.93	15.16	17.19
Al ₂ O ₃	22.55	21.01	22.65
SiO ₂	38.47	39.41	39.15
K ₂ O	10.09	10.34	10.98
CaO	0.00	0.04	0.02
TiO ₂	0.05	0.00	0.31
Cl	0.51	0.72	0.22
MnO	0.00	0.00	0.00
Total	98.00	95.87	97.74
"-O ≡ Cl"	0.12	0.16	0.05
Corrected Total	97.88	95.71	97.69
Fe	0.591	0.594	0.456
Na	0.025	0.015	0.010
Mg	1.927	1.765	1.948
Al	2.031	1.933	2.029
Si	2.939	3.077	2.976
K	0.983	1.030	1.065
Ca	0.000	0.003	0.002
Ti	0.003	0.000	0.018
Mn	0.000	0.000	0.000
Cl	0.066	0.095	0.028
X _{Fe}	0.23	0.25	0.19

Formula recasting on the basis of 22 oxygens. $X_{Fe} = Fe/(Fe+Mg)$.

Table DR2. Chemical composition of glassy inclusions and of ultrapotassic granitic lavas and melts from experimental and natural settings.

Label	1	1*	2	2*	3	3*	4	4*	5	5*	6	7	8	9
Id.	246		8a3		8a4		94a9		94a7					
SiO ₂	77.56	<i>77.27</i>	72.20	<i>72.06</i>	73.26	<i>73.14</i>	74.95	<i>74.78</i>	74.31	<i>74.15</i>	71.41	70.79	76.56	75.76
TiO ₂	0.00	<i>0.00</i>	0.07	<i>0.07</i>	0.02	<i>0.02</i>	0.49	<i>0.49</i>	0.04	<i>0.04</i>	0.28	0.51	0.13	0.19
Al ₂ O ₃	12.25	<i>11.96</i>	13.14	<i>13.00</i>	12.62	<i>12.50</i>	11.40	<i>11.24</i>	11.77	<i>11.61</i>	13.84	13.14	13.58	13.54
Fe ₂ O ₃	0.00	<i>0.00</i>	0.00	<i>0.00</i>	0.00	<i>0.00</i>	0.00	<i>0.00</i>	0.00	<i>0.00</i>	0.00	0.00	1.55	1.08
FeO	0.91	<i>0.91</i>	2.65	<i>2.65</i>	1.47	<i>1.47</i>	1.50	<i>1.50</i>	2.43	<i>2.43</i>	1.78	1.99	0.16	0.12
MnO	0.00	<i>0.00</i>	0.07	<i>0.07</i>	0.04	<i>0.04</i>	0.00	<i>0.00</i>	0.00	<i>0.00</i>	0.03	0.15	0.03	0.02
MgO	0.02	<i>0.02</i>	0.70	<i>0.70</i>	0.58	<i>0.58</i>	0.05	<i>0.05</i>	0.35	<i>0.35</i>	0.39	0.87	0.10	0.04
CaO	0.03	<i>0.03</i>	0.03	<i>0.03</i>	0.33	<i>0.33</i>	0.04	<i>0.04</i>	0.05	<i>0.05</i>	0.15	0.39	0.39	0.88
Na ₂ O	0.73	<i>1.02</i>	0.34	<i>0.48</i>	0.30	<i>0.42</i>	0.41	<i>0.57</i>	0.39	<i>0.54</i>	0.87	0.85	0.76	0.34
K ₂ O	7.56	<i>7.56</i>	7.93	<i>7.93</i>	8.49	<i>8.49</i>	7.13	<i>7.13</i>	7.80	<i>7.80</i>	6.52	6.38	6.80	6.75
P ₂ O ₅	n.a.	<i>n.a.</i>	n.a.	<i>n.a.</i>	n.a.	<i>n.a.</i>	n.a.	<i>n.a.</i>	n.a.	<i>n.a.</i>	0.06	0.07	0.07	0.13
H ₂ O	n.a.	<i>n.a.</i>	n.a.	<i>n.a.</i>	n.a.	<i>n.a.</i>	n.a.	<i>n.a.</i>	n.a.	<i>n.a.</i>	3.06	2.98	0.00	0.80
Total	99.05	<i>98.76</i>	97.13	<i>96.99</i>	97.11	<i>96.99</i>	95.96	<i>95.80</i>	97.13	<i>96.97</i>	98.39	98.12	100.13	99.65
ASI	1.30	<i>1.21</i>	1.43	<i>1.38</i>	1.23	<i>1.19</i>	1.35	<i>1.29</i>	1.28	<i>1.23</i>	1.58	1.46	1.46	1.43
CIPW norm														
Crn	2.83	<i>2.06</i>	3.94	<i>3.58</i>	2.33	<i>2.01</i>	2.95	<i>2.52</i>	2.60	<i>2.20</i>	5.22	4.29	4.43	4.39
Q	43.55	<i>41.58</i>	36.53	<i>35.59</i>	36.21	<i>35.39</i>	44.26	<i>43.15</i>	39.59	<i>38.54</i>	39.36	38.09	45.33	46.37
Or	44.69	<i>44.69</i>	46.86	<i>46.86</i>	50.16	<i>50.16</i>	42.11	<i>42.11</i>	46.10	<i>46.10</i>	38.53	37.70	40.19	39.89
Ab	6.13	<i>8.59</i>	2.91	<i>4.07</i>	2.55	<i>3.56</i>	3.44	<i>4.82</i>	3.26	<i>4.56</i>	7.36	7.19	6.43	2.88
An	0.12	<i>0.12</i>	0.13	<i>0.13</i>	1.64	<i>1.64</i>	0.20	<i>0.20</i>	0.23	<i>0.23</i>	0.35	1.48	1.48	3.52
Q/(Q+Or)	0.49	<i>0.48</i>	0.44	<i>0.43</i>	0.42	<i>0.41</i>	0.51	<i>0.51</i>	0.46	<i>0.46</i>	0.51	0.50	0.53	0.54

1-5: Representative uncorrected EMP analyses of glassy inclusions in garnet. **1*-5*** (italic font): Same as 1-5 but corrected for Na loss (see Morgan and London, 2005) as follows: Na₂O increased of relative 40%; SiO₂ and Al₂O₃ decreased of the calculated Na₂O increase. **6-7:** EMP analyses of experimental (Patiño Douce and Johnston, 1991) glasses from the partial melting of Na-poor pelite at 7 kbar and 950°C, 7 kbar and 950°C, respectively. Na₂O and H₂O calculated by mass balance. **8-9:** XRF analyses of ultrapotassic rhyolites from the Malani Group, India (Maheshwari et al., 1996). ASI = mol Al₂O₃/(CaO+Na₂O+K₂O). Crn, Q, Or, Ab, An = CIPW normative corundum, quartz, orthoclase, albite and anorthite, respectively.

Figure DR1: Simplified geological map of the KKB. Geological sketch map of the Kerala Khondalite Belt, with location of the Koliakkode quarry. Modified after Shabeer (2004).

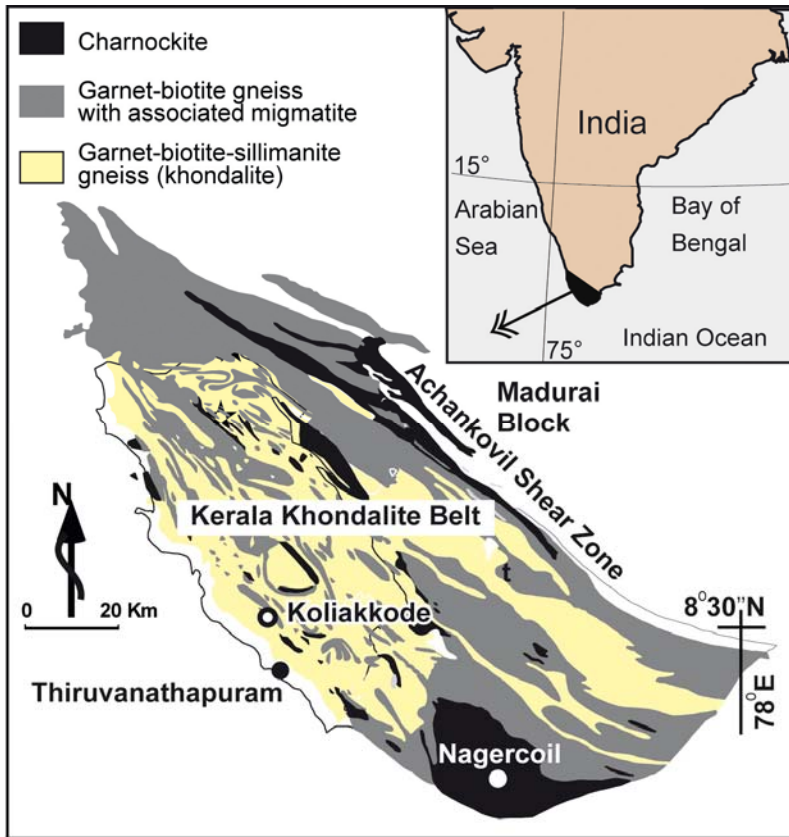
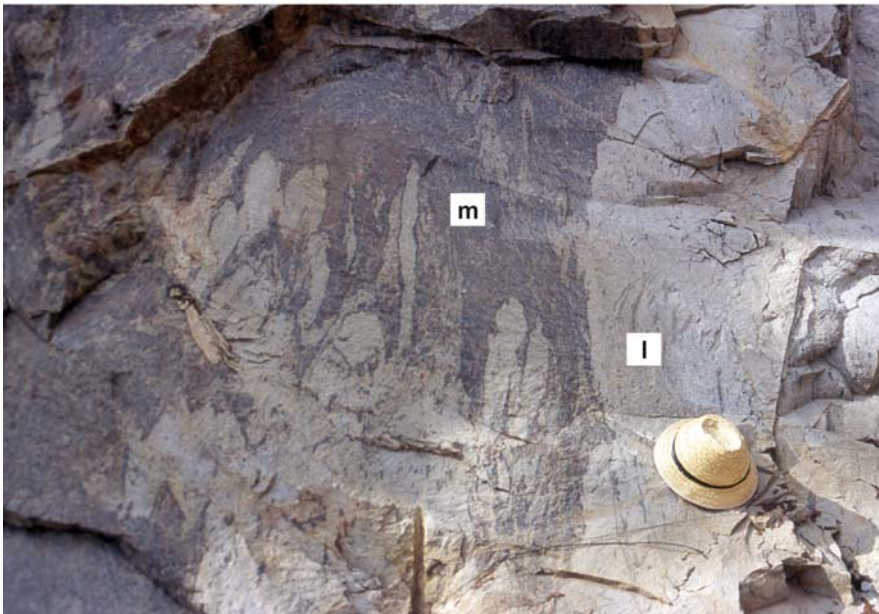


Figure DR2: Outcrop view from Koliakkode quarry. The khondalites here have a typical stromatic diatexite appearance, with extensive segregation of melt from the residual melanosome (m) to form layers and veinlets of leucosome (l) that have been intensely folded. The studied sample comes from the Crd-rich dark melanosome.



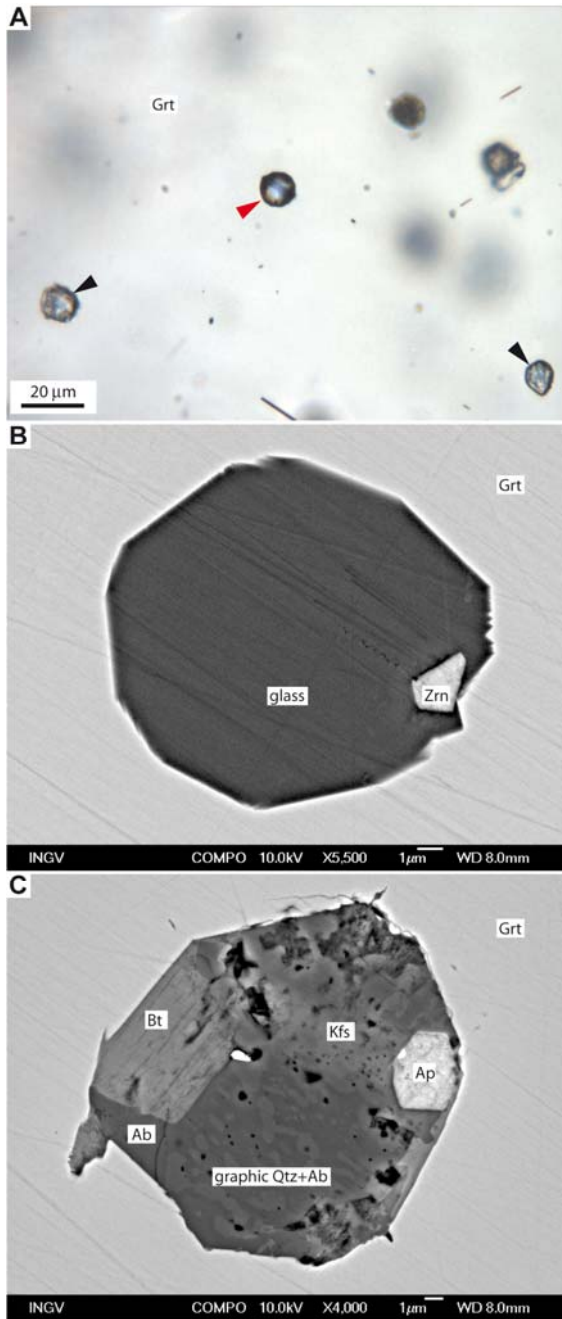


Figure DR3. Further microstructures of melt inclusions in garnet from khondalite.

A, Plane-polarized light photomicrograph of a glassy inclusion (red arrow) coexisting with nanogranite inclusions (black arrows) in a cluster in garnet. **B-C**, Backscattered FESEM images: **B**, One of the largest glassy inclusions found in this study, containing a crystal of zircon. **C**, Nanogranite inclusion showing a coarse biotite, probably crystallized from the garnet wall, and a much finer-grained micrographic Qtz-Ab aggregate occupying large part of the inclusion volume. A diffuse nanoporosity (small black dots) is present in this area and in that occupied by K-feldspar.

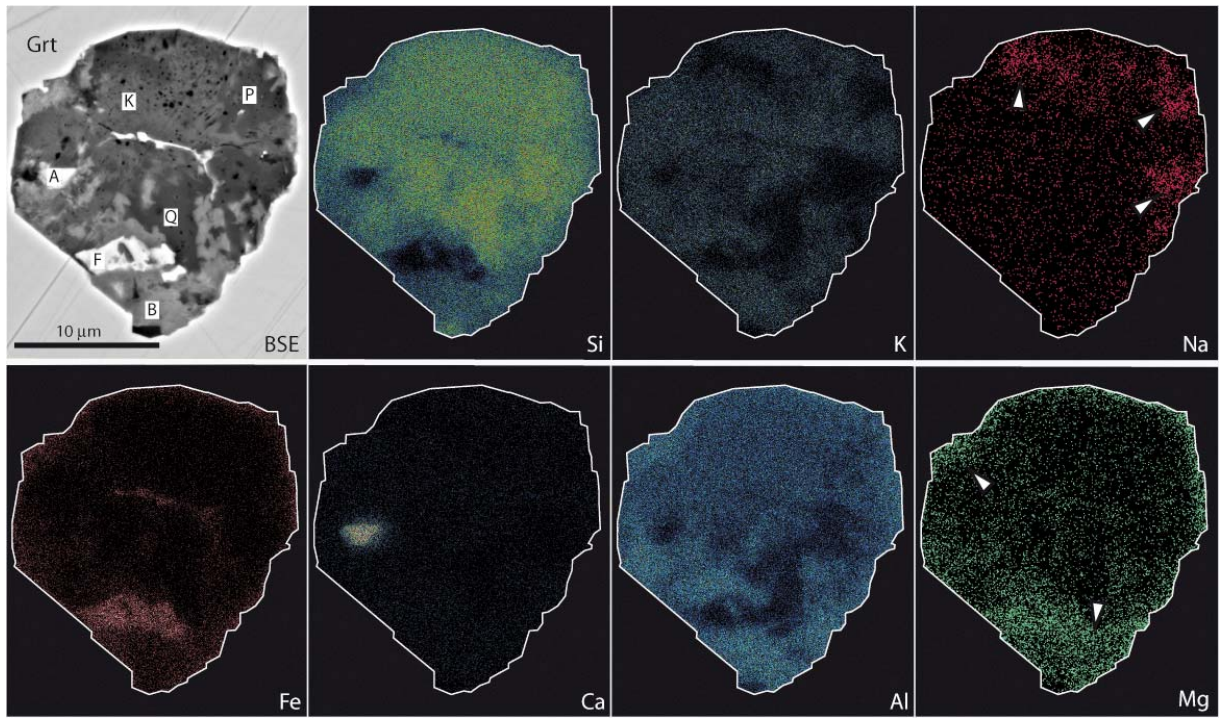


Figure DR4. FESEM BSE image (top left) of an inclusion hosted in garnet, followed by the X-ray maps of elements as labeled. Inclusion contoured (white line) and garnet masked for better visualization. The distribution of elements allows identification of quartz (Q), K-feldspar (K), biotite (B) albitic plagioclase (P), apatite (A) and Fe-Mg oxide (F) in the BSE image.